Pramana – J. Phys. (2021) 95:200
https://doi.org/10.1007/s12043-021-02213-x

Nested multilevel entanglement in Matryoshka states

MRITTUNJOY GUHA MAJUMDAR*

Centre for Excellence in Quantum Technology, Indian Institute of Science, Bengaluru 560012, India
*Corresponding author. E-mail: mrittunjoyg@iisc.ac.in

MS received 29 December 2020; accepted 7 June 2021

Abstract. In this paper, the concept of nested multilevel entanglement is studied and formulated in terms of Matryoshka states. The generation of Matryoshka quantum resource states, which contain nested entanglement patterns, based on an anisotropic XY spin–spin interaction-based model has been proposed. Other classes of nested entanglement, such as in Matryoshka generalised GHZ states and Matryoshka Q-GHZ states, are studied. Generation, characterisation and application of a genuinely entangled seven-qubit resource state close to being a Matryoshka Q-GHZ states is explored, with theoretical schemes for quantum teleportation of arbitrary one-, two- and three-qubits states, bidirectional teleportation of arbitrary two-qubit states and probabilistic circular controlled teleportation proposed for the state. Fractal network protocols, surface codes and graph states as well as generation of arbitrary entangled states at remote locations are also discussed, to highlight the importance of this class of quantum states.

Keywords. Quantum computation; multipartite entanglement; quantum state sharing.

PACS Nos **03.65.Ud; 03.67.-a; 03.67.Lx**

1. Introduction

Quantum entanglement, along with other general non-local quantum correlations, was instrumental in the formulation of information processing tasks in the quantum realm [1–6]. It has been used in applications such as teleportation and superdense coding [7–9]. Bennet *et al* first proposed a scheme for quantum teleportation, wherein a genuinely entangled Bell state was used to transmit an arbitrary single qubit [10]. Different kinds of entangled quantum states have been used to teleport arbitrary quantum states since then, including W states [11,12], Bell states [13,14], GHZ states [15,16] and multiqubit states [17–19]. More recently, various derivatives of the standard teleportation scheme have been proposed, including those used for controlled teleportation [20,21,21], bidirectional teleportation [16,22,23], quantum secret sharing [24–26], quantum operation sharing [27,28] and arbitrated quantum teleportation [29,30].

For multiple participants in a quantum information processing task, multipartite entanglement and entangled multiqubit states play the pre-eminent role, with states varying from GHZ- and W-states to cluster states [31]. Lately, W-GHZ composite states have been used for teleportation, remote state sharing as well as superdense coding of arbitrary quantum states [32,33]. GHZ–GHZ channels have been used for bidirectional quantum communication [34]. Physically, realisation of such composite systems has been explored in varied physical platforms, such as cavity QED [35]. Properties of spin squeezing in a general superposition of multiqubit GHZ state and W state have also been studied [36]. These composite quantum states contain nested entanglement, which can be used for applications in quantum information processing. Yang *et al* investigated the experimental feasibility for creating GHZ states of three logical qubits in a decoherence-free subspace, by using six superconducting transmon qutrits coupled to a one-dimensional co-planar waveguide resonator [37].

Resource theories for entanglement generation and reinforcement of resilience against noise is an important avenue of interest, when it comes to quantum information processing [38–42]. Decoherence-free subspaces provide natural resources to produce robust quantum resource states [43–46]. Stabiliser codes, usually realised on spin chain systems, particularly those

Electronic supplementary material: The online version of this article (https://doi.org/10.1007/s12043-021-02213-x) contains supplementary material, which is available to authorized users.

Published online: 24 November 2021

based on cluster states are resilient quantum systems that are used for measurement-based quantum computation and error corrections [47–49]. The entanglement properties of cluster states generated in array of qubits with Ising-type interactions showed a certain high persistency of entanglement: around half the total number of qubits of the cluster state had to be measured to disentangle the state [50]. The entangling operation defines a resource state in this formalism that is partially entangled in a unique composite-XZ lattice eigenstate. While the entire system is not maximally entangled, the weaker correlation provides segment-wide functionality of the resource state in various segments of the cluster state lattice.

We can extend this idea to generalised states that maintain near-maximal entanglement in segments of the state while maintaining weak entanglement between the segments. The key operative bit here is that of entanglement monogamy, which is a unique feature of quantum correlations that is not present in their classical counterparts. Monogamy restricts the distribution of quantum correlations of a qubit or subsystem with respect to other qubits or subsystems in a multipartite system. If the correlation(s) shared between two or more parties in a multipartite state is lesser than maximal, then they can share some correlations with other parties in the multipartite state. In this manner, monogamy constrains the ways in which entanglement structures can be constructed. For instance, if we begin with a state that is very close to a GHZ state but is not the maximally entangled state itself, we can, in principle superpose these GHZ states in a unique combination of terms.

This is the central idea and motivation behind generalising the concept of Matryoshka states: Matryoshka GHZ-Bell states, Matryoshka generalised GHZ states and Matryoshka Q-GHZ States. The reason for maintaining weak coupling between the near-maximally entangled states is due to the concept of entanglement monogamy, which places restrictions on the amount of entanglement within a segment as well: weaker the coupling, greater is the entanglement within the segments [51–54]. The concept of Matryoshka states was first given by Di Franco *et al* [55], with the name 'Matryoshka' coming from the Russian word for 'nesting doll'. Looking at the various possibilities of mediating the trade-off in entanglement across different layers of qubits, we shall be looking at three classes of Matryoshka states, which are as follows:

1.1 *Matryoshka generalised GHZ states*

$$|\psi_{MGHz}\rangle = \sum_{k=1}^{L} \lambda_k |GHZ_{d_1}^{a_{k,d_1},\pm}\rangle ... |GHZ_{d_N}^{a_{k,d_N},\pm}\rangle \quad (1)$$

$$\times \langle GHZ_{d_i}^{a_{k,d_i},\pm} | GHZ_{d_i}^{a_{k',d_i},\pm}\rangle = \delta_{kk'} \forall i. \quad (2)$$

1.2 *Matryoshka GHZ-Bell states*

$$|\psi_{MGHzB}\rangle = \sum_{k=1}^{L} \lambda_k |GHZ_{d_1}^{a_{k,d_1},\pm}\rangle |B_{d_2}^{a_{k,d_2},\pm}\rangle ... |B_{d_N}^{a_{k,d_N},\pm}\rangle, \quad (3)$$

where $|B\rangle$ signifies a Bell state.

$$\langle GHZ_{d_1}^{a_{k,d_1},\pm} | GHZ_{d_1}^{a_{k',d_1},\pm}\rangle = \delta_{kk'} \forall i \quad (4)$$

$$\langle B_{d_i}^{a_{k,d_i},\pm} | B_{d_i}^{a_{k',d_i},\pm}\rangle = \delta_{kk'} \forall i. \quad (5)$$

1.3 *Matryoshka Q-GHZ states*

$$|\psi_{MExG}\rangle = \sum_{k=1}^{L} \lambda_k |A_1^k\rangle |GHZ_{d_2}^{a_{k,d_2},\pm}\rangle ... |GHZ_{d_N}^{a_{k,d_N},\pm}\rangle \quad (6)$$

$$\langle GHZ_{d_i}^{a_{k,d_i},\pm} | GHZ_{d_i}^{a_{k',d_i},\pm}\rangle = \delta_{kk'} \forall i, \langle A_1^k | A_1^{k'}\rangle = \delta_{kk'}, \quad (7)$$

where $|A\rangle$ are orthogonal states that are eigenstates in the Z-basis for all qubits in the state.

Here the subscript d_i in $|GHZ_{d_i}^{a_{k,d_i}}\rangle$ denotes the number of qubits in the ith subsystem, while a is the decimal representation of the first term in the GHZ-like state and $\pm$ denotes the relative phase between the terms in superposition. GHZ-like states are all those states that can be created from the GHZ state using local unitary operations. So, for instance, in a three-qubit system $|GHZ^{2,+}\rangle = \frac{1}{\sqrt{2}}(|010\rangle + |101\rangle)$. A point to note here is that the subsystems can comprise any arbitrary number of qubits, and a depends on the index of superposition and number of qubits in the subsystem. $L = 2^{n_h}$ where n_h is the number of qubits in the largest subsystem. Also, the Bell states can be considered as the GHZ-like states for $d = 2$, due to which the Matryoshka GHZ-Bell states can be regarded as an instance of asymmetric Matryoshka generalised GHZ state, where the number of qubits in the subsystems are not equal across the state.

In this paper, we shall be discussing the generation, particularly using the schematic shown in figure 1, and application of Matryoshka states to quantum information processing.

2. Generation of Matryoshka states

We can generate Matryoshka states using multiple physical platforms. Two of them are spin systems and

trapped ions. Previously, Fröwis and Dür [56] studied the stability of superpositions of macroscopically distinct quantum states under decoherence, focussing on the realisation of concatenated-GHZ states: $|\phi_C\rangle = \frac{1}{\sqrt{2}}(|GHZ_m^+\rangle^{\otimes N} + |GHZ_m^-\rangle^{\otimes N})$ (with $|GHZ_N^{\pm}\rangle = \frac{1}{\sqrt{2}}(|0\rangle^{\otimes N} \pm |1\rangle^{\otimes N})$), which is a Matryoshka generalised state in trapped ion systems. In this paper, the generalised generation of Matryoshka states will be explored in spin systems in condensed matter physics. We consider N spin-$\frac{1}{2}$ particles, with each spin coupled to its nearest neighbours by the XY Hamiltonian

$$H = \sum_{i=1}^{N-1}(J_{X,i}\hat{X}_i\hat{X}_{i+1} + J_{Y,i}\hat{Y}_i\hat{Y}_{i+1}), \tag{8}$$

where $J_{\sigma,i}$ is the pairwise coupling constant with $\sigma = \hat{X}, \hat{Y}, \hat{Z}$ being the Pauli operators. For this paper, we take N to be odd. Franco *et al* [55] showed that it is sufficient to state that the information flux between the $\hat{X}$ ($\hat{Y}$) operators of the first and last qubits in the spin chain depends on an alternating set of coupling strengths. For example, the information flux from $\hat{X}_1$ to $\hat{X}_N$ depends only on the set $\{J_{Y,1}, J_{X,2}, ..., J_{Y,N-1}\}$ and is independent of any other coupling rate in the spin chain. Christandl *et al* [57,58] showed that after a time $t^* = \pi/\lambda$ with λ being a scaling constant (as mentioned in the definition of the case of a perfect state transfer in a linear spin chain given by weighted coupling strengths: $J_{\sigma,i} = \lambda\sqrt{i(N-i)}$), the state of the first qubit in the spin chain can be perfectly transferred to the last qubit. We see that by preparing the initial state of this spin chain in a completely separable eigenstate of the tensorial product of Z_i operators, say $|\Psi(0)\rangle = |000...0\rangle_{12...N}$, we obtain an information flux towards symmetric two-site spin operators, and a final state of the form [55]

$$|\psi_0\rangle = |0\rangle_c \otimes_{i=0}^{M} |\psi_+\rangle_{2i+1,N-2i} \otimes_{i=1}^{M} |\psi_-\rangle_{2i,N-2i+1}, \tag{9}$$

$$|\psi_1\rangle = |1\rangle_c \otimes_{i=0}^{M} |\psi_-\rangle_{2i+1,N-2i} \otimes_{i=1}^{M} |\psi_+\rangle_{2i,N-2i+1}, \tag{10}$$

where c labels the central site of the spin chain, $M = (N-3)/4$ and $|\psi_\pm\rangle = (1/\sqrt{2})(|00\rangle \pm |11\rangle)$. An illustration of the set-up is shown in figure 2.

The critical step in the creation of the Matryoshka GHZ-Bell state is the evolution of the central and two neighbouring qubits to the GHZ state, without disturbing the rest of the spin chain. This is a key result around the generation of Matryoshka GHZ-Bell states in this paper, which can be extended to other classes of Matryoshka states. For this, we need to switch off all the interactions except for those connecting the central qubit to the neighbouring ones. A point to note here is that had we started with $|\Psi(0)\rangle = |111...1\rangle_{12...N}$, and we would have obtained a final state of the form

$$|\psi_0\rangle = |0\rangle_c \otimes_{i=0}^{M} |\psi_-\rangle_{2i+1,N-2i} \otimes_{i=1}^{M} |\psi_+\rangle_{2i,N-2i+1} \tag{11}$$

$$|\psi_1\rangle = |1\rangle_c \otimes_{i=0}^{M} |\psi_+\rangle_{2i+1,N-2i} \otimes_{i=1}^{M} |\psi_-\rangle_{2i,N-2i+1}. \tag{12}$$

We use this principle and the idea that after evolution over time t^*, the states in eqs (2) and (3) transform back to $|000...000\rangle_{12...N}$ and states in eqs (4) and (5) transform back to $|111...11\rangle_{12...N}$. We can utilise this concept, by taking the state in eq. (2) and evolving it, for the truncated subsystem comprising the central qubit and the adjoining qubits. A point to note here is that due to only coupling that connects to the central qubits, the coupling strength ($J'_{\sigma,i} = \lambda'\sqrt{i(3-i)}$) and time of evolution ($t'' = \pi/\lambda'$) vary accordingly. Before carrying out this evolution, we perform a Hadamard operation on the central qubit to give

$$|\psi_0\rangle = \frac{1}{\sqrt{2}}(|0\rangle_c + |1\rangle_c) \otimes_{i=0}^{M} |\psi_+\rangle_{2i+1,N-2i} \otimes_{i=1}^{M} |\psi_-\rangle_{2i,N-2i+1}. \tag{13}$$

We now perform the truncated subsystem time evolution with the parameters (J', t'') to give us the state

$$|\psi_0\rangle = \frac{1}{\sqrt{2}}(|000\rangle + |111\rangle)_{c-1,c,c+1} \otimes_{i=0}^{M-1} |\psi_+\rangle_{2i+1,N-2i} \otimes_{i=1}^{M} |\psi_-\rangle_{2i,N-2i+1}. \tag{14}$$

Therefore, we can obtain a Matryoshka GHZ-Bell state using nearest spin-spin interactions in a spin chain. A similar generation protocol can be defined for the other two classes of Matryoshka states. The teleportation of an arbitrary n-qubit state can be performed using Matryoshka GHZ-Bell states [7].

Given the triangular three-qubit configuration, we can also consider the anisotropic Heisenberg Hamiltonian, which describes the interaction between three spins that are located at the corners of an equilateral triangle lying in the xy-plane, as shown in figure 1.

$$H = -J_{xy}\sum_{i=1}^{3}(S_i^x S_{i+1}^x + S_i^y S_{i+1}^y) - J_z\sum_{i=1}^{3} S_i^z S_{i+1}^z + H_z, \tag{15}$$

where the three spins S_i, with $S = 1/2$, are located at the corners $i = 1, 2, 3$, and $S_1 = S_4$. J_{xy} and J_z are the in-plane and out-of-plane exchange coupling constants respectively, and $H_Z = \sum_{i=1}^{3} b_i$. S_i denotes the Zeeman coupling of the spins S_i to the externally applied magnetic fields b_i at the sites i. If we consider

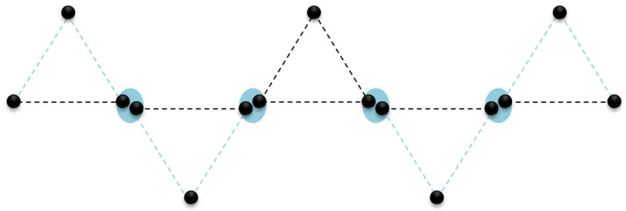

Figure 1. Schematic for all (three) classes of Matryoshka states explored in this paper. The triangular formations encapsulate the logical units of two/three qubits mediated by CNOT gates. Each of these triangular units are weakly coupled to each other (shown with light blue patches). In the case of the Matryoshka GHZ-Bell states, we only have the black links, while for the Matryoshka generalised GHZ states and Matryoshka Q-GHZ states, we also have the blue links.

isotropic exchange couplings: $J_{xy} = J_z = J > 0$ (ferromagnetic coupling) and $b_i = 0 \forall i$, we have a ground-state quadruplet that is spanned by the GHZ states: $\frac{1}{\sqrt{2}}(|000\rangle + |111\rangle)$ and $\frac{1}{\sqrt{2}}(|000\rangle - |111\rangle)$, along with the W- and spin-flipped W-states. A set of appropriately chosen magnetics fields will allow us to split off an approximate GHZ state from this degenerate eigenspace. If we find a set of magnetic fields that, in classical spin systems, shall result in exactly two degenerate minima for the configurations $|000\rangle$, representing the $\downarrow\downarrow\downarrow$ spin configuration, and $|111\rangle$, representing the $\uparrow\uparrow\uparrow$ spin configuration, with an energy barrier in between, quantum mechanical tunnelling shall yield the desired states. The magnetic fields must be of the same strength, in-plane and sum to zero, with a convenient additional choice being that of the field pointing radially outward. Therefore, the successive directions of the magnetic fields have to differ by an angle of $2\pi/3$ with respect to each other. Going by the schematic in figure 1, we can write the Hamiltonian

$$
\begin{aligned}
H = & -J_{xy}\sum_{i=1}^{3}(S_i^x S_{i+1}^x + S_i^y S_{i+1}^y) - J_z\sum_{i=1}^{3} S_i^z S_{i+1}^z \\
& + H_z + \sum_{il=1}^{N_l}\Bigg[- J_{xy}^{(il)}\sum_{i=1}^{3}(S_i^x S_{i+1}^x + S_i^y S_{i+1}^y) \\
& - J_z^{(il)}\sum_{i=1}^{3} S_i^z S_{i+1}^z + H_z^{(il)}\Bigg] \\
& + \sum_{ir=1}^{N_r}\Bigg[- J_{xy}^{(ir)}\sum_{i=1}^{3}(S_i^x S_{i+1}^x + S_i^y S_{i+1}^y) \\
& - J_z^{(ir)}\sum_{i=1}^{3} S_i^z S_{i+1}^z + H_z^{(ir)}\Bigg] \\
& + \sum_{il=1}^{N_l}\lambda^{l}_{(il,il+1)} S_i^{n_r}\cdot S_{i+1}^{n_l} \\
& + \sum_{ir=0}^{N_r-1}\lambda^{r}_{(ir,ir+1)} S_i^{n_r}\cdot S_{i+1}^{n_l}, \qquad (16)
\end{aligned}
$$

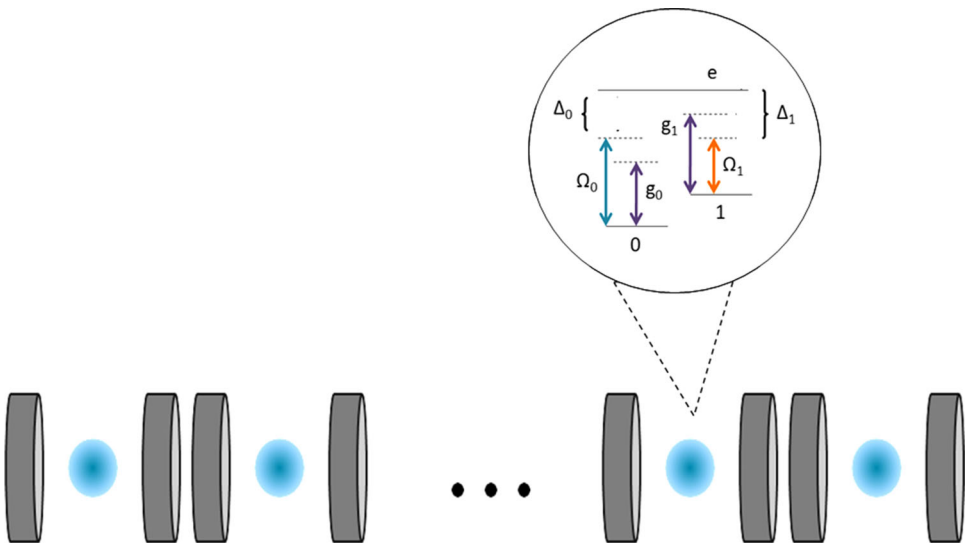

Figure 2. Scheme for the generation of Matryoshka GHZ-Bell resource states, where the effective spin–spin *XY* Hamiltonianan is obtained as an effective adiabatic Hamiltonian for a linear chain of optical cavities with each interacting with a three-level atomic system. The ground states of each atomic unit provide the computational space of each spin, and the dipole-forbidden transition between these states is realised as an (adiabatic) Raman transition through the excited state: $|e\rangle_i$ with $i = 1, 2, ..., N$. The cavity field drives off-resonantly the dipole-allowed channel $|j\rangle_i \leftrightarrow |e\rangle_i$ with the Rabi frequency g_j, $j = 0, 1$. Two lasers are also coupled to these atomic transitions with strength Ω_j and detuning Λ_j.

where the superscripts il and ir denote the left and right branches respectively of the schematic around a central triangular unit. For $il = 1$, we have the left-most triangular unit and for $ir = N_r$, we have the right-most triangular unit. N_l and N_r denote the number of units on the left and right sides of the central triangular unit. In principle, we can have an asymmetric case where $N_l \neq N_r$. In the fourth line, the term S_{N_l+1} and S_0 refer to the spins in the central triangular unit connected to the adjacent left and right triangular units respectively. Moreover, both $\lambda^l_{(il,il+1)}$ and $\lambda^l_{(ir,ir+1)}$ are coupling constants between adjacent triangular units that are numerically negligible with respect to J but are non-zero, to account for interunit coupling. $S_i^{n_r}$ and $S_i^{n_l}$ are the right and left connecting nodes of the ith triangular unit.

An important point here is the condition: $\langle GHZ_{d_i}^{a_{k,d_i},\pm}|GHZ_{d_i}^{a_{k',d_i},\pm}\rangle = \delta_{kk'}\forall i$, $\langle A_1^k|A_1^{k'}\rangle = \delta_{kk'}$ in eqs (2), (4) and (7). This is ensured by the additional application of single qubit gates on the nodes of the triangular units. For instance,

$$\frac{1}{\sqrt{2}}(|000\rangle + |111\rangle) \xrightarrow{\sigma_x^2} \frac{1}{\sqrt{2}}(|010\rangle + |101\rangle).$$

Using a combination of such single qubit operations, we can span the entire space of GHZ and GHZ-like states. The important point here is the synchronised timing of these operations, with the interunit coupling, so as to give us a superposition over orthogonal GHZ and GHZ-like states for all triangular units, as shown in figure 1.

3. Tesselation of Matryoshka states

The Matryoshka generalised GHZ states can also be oriented in a tesselated manner, as shown in figure 3a for the case of symmetric 3-qubit GHZ triangular units. The Matryoshka GHZ-Bell states, a specific form of these states, can even be oriented in an emanatory manner, as shown in figure 3b. These two orientations can be used for tessellation in three dimensions, as in the case of the spherical configuration shown in figure 3c, which shows the method of lattice surgery (discussed later in the paper). More complex forms such as the hexagonal–pentagonal tiling with 6-qubit and 5-qubit GHZ states can be used for forms such as truncated icosahedrons. Lastly, we can also have higher GHZ-forms in a self-similar, fractal manner, as shown in figure 3d. Each of these configurations will be studied in the *Application* section of this paper. An interesting future direction of pursuing this line of research would be in squeezed baths, which Zippilli *et al* studied and it is showed that a squeezed bath, which acts on the central element of a harmonic chain, could drive the entire system to a steady state that features a series of nested entangled pairs of oscillators [59]. This series ideally covers the entire chain regardless of its size. Extending this result to higher number of nearest-neighbour interactions is non-trivial.

4. Applications of Matryoshka states

Matryoshka states have a second level of entanglement (nesting) and have additional protection against loss of coherence under local transformations.

4.1 *Fractal network protocol*

In this paper, a new quantum communication architecture is being proposed, whereby there are levels of entanglement which underly a distributed network. If we have

$$|0\rangle_L^n = \frac{1}{\sqrt{2}}(|0_L^{n-1}0_L^{n-1}0_L^{n-1}\rangle + |1_L^{n-1}1_L^{n-1}1_L^{n-1}\rangle) \quad (17)$$

$$|1\rangle_L^n = \frac{1}{\sqrt{2}}(|0_L^{n-1}0_L^{n-1}0_L^{n-1}\rangle - |1_L^{n-1}1_L^{n-1}1_L^{n-1}\rangle). \quad (18)$$

As you can see, these are special cases of Matryoshka generalised GHZ states, with the superscript n defining the layer of the network. A point to note here is that $n = 1$ is the layer with physical qubits, and so $|0\rangle_L^1 = |0\rangle$ and $|1\rangle_L^1 = |1\rangle$. This effectively creates layers of entangled entanglement. This is highly useful in providing multiple levels of protection in quantum network encoding. The key point here is the heralded nature in which we can access levels from the highest to the lowest, with a projective measurement onto the basis logical qubits of the just-lower level of entanglement to pass through a level of entanglement-enabled security and robustness.

4.2 *Surface codes, graph states and cluster states*

We can define effective surface codes with Matryoshka states, with triangular units. The primary operation proposed to be utilised in this regard is that of lattice surgery and merging. Topological encoding of quantum data facilitates information processing to be protected from the effects of decoherence on physical qubits, by having a logical qubit encoded in the entangled state of many physical qubits. Among the various codes used for this purpose, the surface code has the highest tolerance of component error, when implemented on a two-dimensional lattice of spin-qubits with nearest-neighbour interactions [60–64]. Mhalla and Perdrix [65] proved that the application of measurements in the

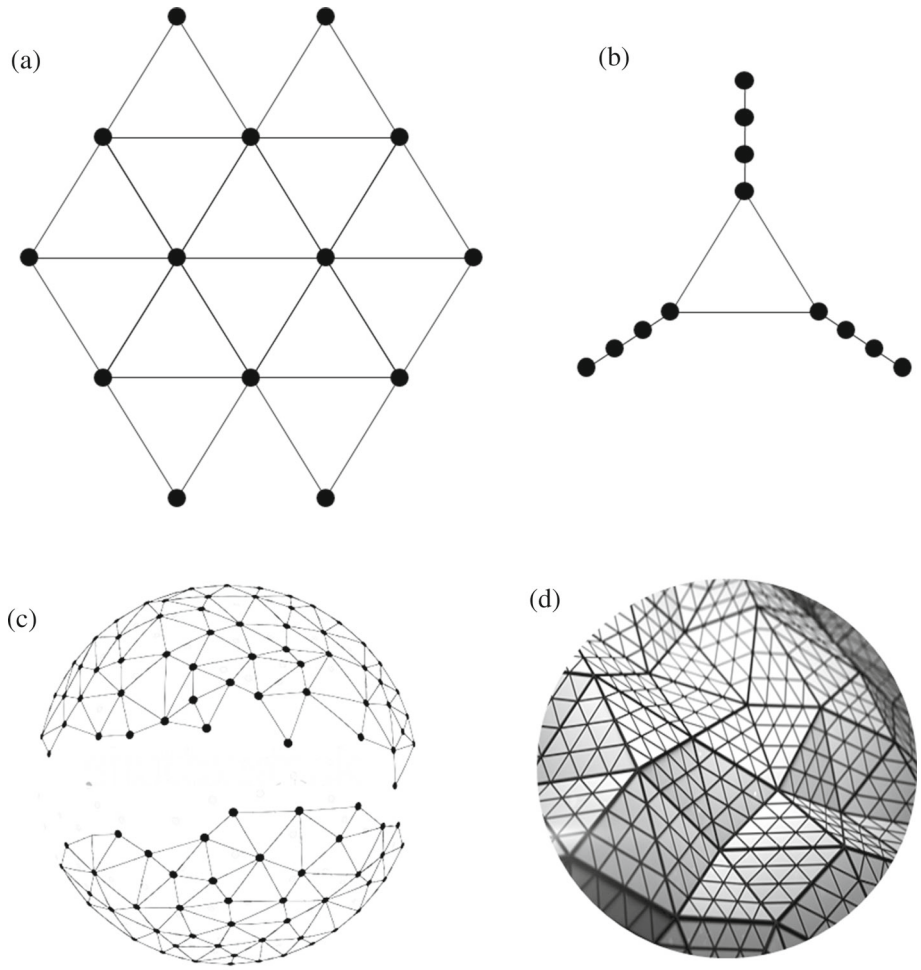

Figure 3. The various tesselation patterns possible with the GHZ triangular units in (a) Generalised GHZ states in a planar tesselated format, (b) GHZ-Bell States with an emanatory geometry, (c) spherical pattern created by planar codes, along with illustration of lattice surgery with projective measurements, and (d) hierarchical GHZ-state levels, where we have a self-similar nature of the tesselation. A point to note here is that each node in the diagram has three physical qubits (one from each GHZ triangular unit) in the Generalised GHZ states and two physical qubits in the GHZ-Bell states.

(X, Z) plane, with one-qubit measurement as per the basis

$$\{\cos\theta|0\rangle + \sin\theta|1\rangle, \sin\theta|0\rangle - \cos\theta|1\rangle\} \tag{19}$$

for some θ over graph states that are represented by triangular grids, is a universal model of quantum computation. A point to note here is that, for any θ, the observable associated with the measurement in this basis is $\cos 2\theta Z + \sin 2\theta X$. For a given simple undirected graph $G = (V, E)$ of order n, where V represent the vertices and E the edges, the graph state $|G\rangle$ is the unique quantum state such that for any vertex $u \in V$,

$$X_u Z_{\mathcal{N}(u)}|G\rangle = |G\rangle. \tag{20}$$

The Pauli operators constituting a group acting on a set V of n qubits is generated by $X_u, Z_u, i \cdot I_{u\in V}$, where I is the identity, X_u and Z_u are operators that act as identity on the neighbourhood of u and with the following action on vertex u:

$$X : |x\rangle \rightarrow |\overline{x}\rangle \tag{21}$$

$$Z : |x\rangle \rightarrow (-1)^x|\overline{x}\rangle. \tag{22}$$

In our circuit, we shall have to project three physical qubits from three adjacent triangular units to a single subspace for implementing this model. If we consider the state

$$\frac{1}{2\sqrt{2}}(|00_c0\rangle + |11_c1\rangle)(|00_c0\rangle + |11_c1\rangle)(|00_c0\rangle + |11_c1\rangle),$$

with the subscript c denoting the physical qubits adjacent to each other and that are projected to a single subspace. If we initialise an ancilla qubit in the state

$$|+\rangle = \frac{1}{\sqrt{2}}(|0\rangle + |1\rangle)$$

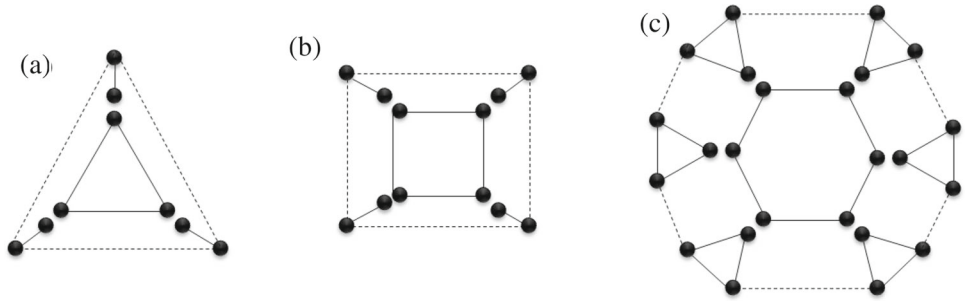

Figure 4. Illustration of networks for entanglement generation in remote nodes in (a) triangular format (b) rectangular format (c) polyhedra (dodecagon) format, with distinct patterns of entanglement generated at the periphery depending on the projective measurements at the central terminal(s).

and use the conditional rotation gate

$$U_\gamma = \begin{pmatrix} 1 & 0 & 0 & 0 \\ 0 & 1 & 0 & 0 \\ 0 & 0 & \cos\frac{\gamma}{2} & \sin\frac{\gamma}{2} \\ 0 & 0 & -\sin\frac{\gamma}{2} & \cos\frac{\gamma}{2} \end{pmatrix} \tag{23}$$

and apply this sequentially with the three adjacent physical qubits (with subscript c) and the ancilla as the target, we project the ancilla to a unique state that can be retained for the graph state that is thereby defined, by going over the entire tessellated lattice of triangular GHZ-units.

4.3 *Establishing multiparticle entanglement between nodes of a quantum communication network*

We can use the unique form of the asymmetric Matryoshka generalised GHZ states to establish multipartite entanglement between nodes of a quantum communication network. The important part about this protocol is the role of projection measurements on a central terminal. Some of the nodal orientations that can be utilised for the same are shown in figure 4. Considering a Matryoshka GHZ-Bell state with an m-particle GHZ state and n-terminals in a quantum network

$$|\psi_{MGHzB}\rangle = \sum_{k=1}^{L} \lambda_k |GHZ_m^{a_{k,m},\pm}\rangle |B_{d_1}^{a_{k,d_1},\pm}\rangle ... |B_{d_n}^{a_{k,d_n},\pm}\rangle, \tag{24}$$

where $|B\rangle$ signifies a Bell-state, $\langle GHZ_m^{a_{k,m},\pm}|GHZ_m^{a_{k',m},\pm}\rangle = \delta_{kk'}\forall i$ and $\langle B_{d_i}^{a_{k,d_i},\pm}|B_{d_i}^{a_{k',d_i},\pm}\rangle = \delta_{kk'}\forall i$. Each user has one particle of a Bell-state, while the other particle of the Bell-state is with the central terminal. Measuring the particles of the Bell-pairs at the central terminal in a basis defined by maximally entangled states over n-qubits will project the distant qubits into maximally n-qubit entangled states as well. In fact, it need not only be one n-qubit maximally entangled state at the spatially distant nodes but could be multiple (partially or maximally) entangled states of varying number of qubits connecting different permutations of end terminals, depending on the projective measurement performed on the central terminal.

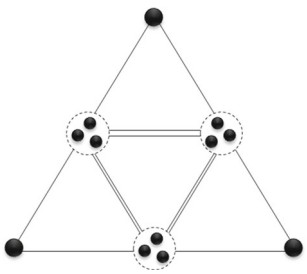

Figure 5. Network repeater protocol with three-qubit projective measurements at nodes to create higher-distance entangled networks.

4.4 *Quantum networks, repeater protocols and quantum communication*

Quantum networks can facilitate the realisation of quantum technologies such as distributed quantum computing [66], secure communication schemes [67] and quantum metrology [68–71]. In our formalism for GHZ-based network protocols, the key element is that of being able to merge GHZ triangular units, which is done by projecting states at adjacent nodes into a single subspace, as has been tried on atomic systems previously [72]. An illustrative nodal structure, along with the operative procedural elements, for network repeater protocol with three-qubit projective measurements at nodes to create higher-distance entangled network is shown in figure 5.

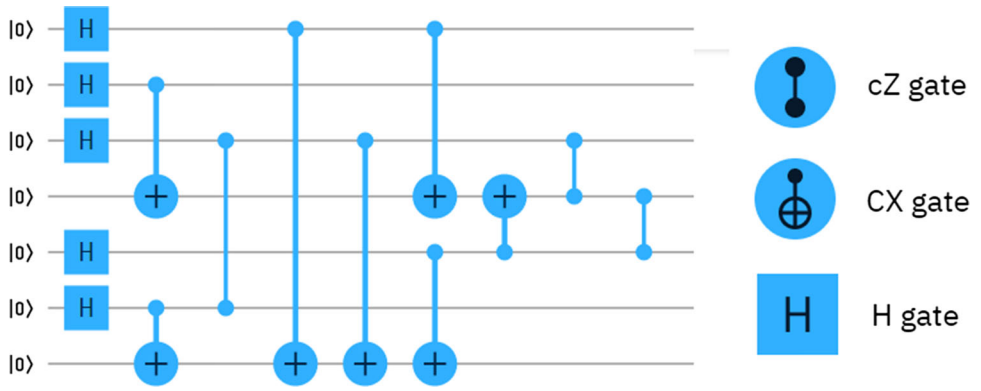

Figure 6. Quantum Circuit for the generation of the seven-qubit genuinely entangled state, on *IBM Quantum Experience*. Here *CX gate* is the CNOT gate, *cZ gate* is the CPHASE gate and *H gate* is the Hadamard gate.

This operation is realised by reading out the atomic excitations and directing the emitted light fields to the swapping station described above (see also the inset of figure 2a), where success is heralded by the detection of a single photon (see §A of Supplementary material for details). Otherwise the resulting state is discarded.

4.5 *Teleportation and superdense coding*

Let us look at the applications of such nested entanglement with the example of a state close to a Matryoshka Q-GHZ state: the Xin-Wei Zha (XZW) State. Xin-Wei Zha *et al* [73] discovered a genuinely entangled seven-qubit state through a numerical optimisation process, following the path taken by Brown *et al* [74] and Borras *et al* [75] to find genuinely entangled five-qubit and six-qubit states:

$$\begin{aligned}|\psi_7\rangle \;=\; & \frac{1}{2\sqrt{2}}(|000\rangle_{135}|\psi_+\rangle_{24}|\psi_+\rangle_{67} \\ & +|001\rangle_{135}|\phi_-\rangle_{24}|\phi_+\rangle_{67}+|010\rangle_{135}|\psi_-\rangle_{24}|\phi_-\rangle_{67} \\ & +|011\rangle_{135}|\phi_+\rangle_{24}|\psi_-\rangle_{67}+|100\rangle_{135}|\phi_+\rangle_{24}|\phi_+\rangle_{67} \\ & +|101\rangle_{135}|\psi_-\rangle_{24}|\psi_+\rangle_{67}+|110\rangle_{135}|\phi_-\rangle_{24}|\psi_-\rangle_{67} \\ & +|111\rangle_{135}|\psi_+\rangle_{24}|\phi_-\rangle_{67}). \qquad (25)\end{aligned}$$

This state is a specific form of the Q-GHZ state defined in eq. (6), with $\lambda_k \forall k = (1/2\sqrt{2})$ and $|A_1^k \in \{|000\rangle, |001\rangle, |010\rangle, |011\rangle, |100\rangle, |101\rangle, |110\rangle, |111\rangle\}$. Another point to note here is that the GHZ states here are for $d = 2$, thereby effectively being the Bell-states. This resource state can be used for teleportation of arbitrary single, double and triple qubit states.

The 3 (Q State)-2 (Bell State)-2 (Bell State) structure of the resource-state, given in eq. (17), helps us in devising a quantum circuit to generate the state, as shown in figure 6 and realised on IBM quantum experience. To obtain the resource state, we apply a unitary operator on qubits 1, 3 and 5: $U = I_{4\times4} \oplus (\sigma_z \otimes \sigma_z)$.

This state has marginal density matrices for subsystems over one or two qubits that are completely mixed, with $\pi_{ij} = Tr_{ij}\rho_{ij}^2 = \frac{1}{4} \forall i, j \in \{1, 2, 3, 4, 5, 6, 7\}, i < j$, $\pi_i = Tr_i\rho_i^2 = \frac{1}{2} \quad \forall \quad i \in \{1, 2, 3, 4, 5, 6, 7\}$. For three-qubit subsystems, some of the partitions have mixed marginal density matrices: $\pi_{ijk} = Tr_{ijk}\rho_{ijk}^2 = \frac{1}{8} \quad \forall \quad i, j \in \{1, 2, 3, 4, 5, 6, 7\}, i < j < k \wedge (ijk) \neq (127), (367), (457)$ and $\pi_{127} = \pi_{367} = \pi_{457} = \frac{1}{4}$.

The seven-qubit genuinely entangled resource state $|\Gamma_7\rangle$ can be used for a number of applications, such as quantum secret sharing, the perfect linear teleportation of an arbitrary one-qubit state, probabilistic circular teleportation of arbitrary one-qubit states, perfect linear teleportation of an arbitrary two-qubit state, bidirectional teleportation of arbitrary two-qubit states and perfect linear teleportation of an arbitrary three-qubit state (see supplementary material).

5. Conclusion

In this paper, the generation and application of nested entanglement in Matryoshka resource states for quantum information processing was studied. A novel scheme for the generation of such quantum states has been proposed using an anisotropic XY spin–spin interaction-based model. The application of the Matryoshka GHZ-Bell states for n-qubit teleportation is reviewed and an extension of this formalism to more general classes of Matryoshka states is posited. An example of a state close to a perfect Matryoshka Q-GHZ state is given in the form of the genuinely entangled seven-qubit Xin-Wei Zha state. Generation, characterisation and application of this seven-qubit resource state are presented. This work should lay the groundwork for other studies into the area of nested entanglement, including forays into higher layers of nesting entanglement.

Acknowledgements

The author would like to acknowledge the guidance and contribution of Prof. Prasanta Panigrahi, IISER-Kolkata. This work was supported by the Homi Bhabha Centre for Science Education, Tata Institute of Fundamental Research, Mumbai, India.

References

[1] R Horodecki, P Horodecki, M Horodecki and K Horodecki, *Rev. Mod. Phys.* **81**(**2**), 865 (2009)
[2] J Barrett, N Linden, S Massar, S Pironio, S Popescu and D Roberts, *Phys. Rev. A* **71**(**2**), 022101 (2005)
[3] C H Bennett and D P DiVincenzo, *Nature* **404**(**6775**), 247 (2000)
[4] U Khalid, J ur Rehman and H Shin, *Sci. Rep.* **10**(**1**), 1 (2020)
[5] M G Majumdar, *Quantum Inf. Process.* **19**(**10**), 1 (2020)
[6] M G Majumdar, *J. Quantum Inf. Sci.* **8.4**, 139 (2018)
[7] D Saha and P K Panigrahi, *Quantum Inf. Process.* **11**(**2**), 615 (2012)
[8] M-J Zhao, Z-G Li, X Li-Jost and S-M Fei, *J. Phys. A* **45**(**40**), 405303 (2012)
[9] Z Zhang, L Shu and Z Mo, *Quantum Inf. Process.* **12**(**5**), 1957 (2013)
[10] C H Bennett, G Brassard, C Crépeau, R Jozsa, A Peres and W K Wootters, *Phys. Rev. Lett.* **70**(**13**), 1895 (1993)
[11] X Gao, Z Zhang, Y Gong, B Sheng and X Yu, *JOSA B* **34**(**1**), 142 (2017)
[12] B-S Shi and A Tomita, *Phys. Lett. A* **296**(**4–5**), 161 (2002)
[13] W Tian-Yin and W Qiao-Yan, *Chin. Phys. B* **20**(**4**), 040307 (2011)
[14] X Tan, X Li and P Yang, *Comput. Mater. Contin.* **57**(**3**), 495 (2018)
[15] J Dong and J F Teng, *The Eur. Phys. J. D* **49**(**1**), 129 (2008)
[16] S Hassanpour and M Houshmand, *Quantum Inf. Process.* **15**(**2**), 905 (2016)
[17] P Espoukeh and P Pedram, *Quantum Inf. Process.* **13**(**8**), 1789 (2014)
[18] R-G Zhou, C Qian and H Ian, *IEEE Access* **7**, 42445 (2019)
[19] A Kumar, S Adhikari, S Banerjee and S Roy, *Phys. Rev. A* **87**(**2**), 022307 (2013)
[20] F-G Deng, C-Y Li, Y-S Li, H-Y Zhou and Y Wang, *Phys. Rev. A* **72**(**2**), 022338 (2005)
[21] F Yan and D Wang, *Phys. Lett. A* **316**(**5**), 297 (2003)
[22] V Sharma, C Shukla, S Banerjee and A Pathak, *Quantum Inf. Process.***14**(**9**), 3441 (2015)
[23] Y-J Duan, X-W Zha, X-M Sun and J-F Xia, *Int. J. Theor. Phys.* **53**(**8**), 2697 (2014)
[24] M Hillery, V Bužek and A Berthiaume, *Phys. Rev. A* **59**(**3**), 1829 (1999)
[25] L Xiao, G L Long, F-G Deng and J-W Pan, *Phys. Rev. A* **69**(**5**), 052307 (2004)
[26] D Gottesman, *Phys. Rev. A* **61**(**4**), 042311 (2000)
[27] Z Zhang and C-Y Cheung, *J. Phys. B* **44**(**16**), 165508 (2011)
[28] Q Ji, Y Liu, X Yin, X Liu and Z Zhang, *Quantum Inf. Process.* **12**(**7**), 2453 (2013)
[29] J Heo, C-H Hong, M-S Kang, H Yang, H-J Yang, J-P Hong and S-G Choi, *Sci. Rep.* **7**(**1**), 1 (2017)
[30] T Zheng, Y Chang and S-B Zhang, *Quantum Inf. Process.* **19**, 1 (2020)
[31] M Walter, D Gross and J Eisert, Multipartite entanglement. *Quantum Information: From Foundations to Quantum Technology Applications*, pp 293–330 (2016)
[32] T Dash, SK Rajiuddin and P K Panigrahi, *Opt. Commun.* **464**, 125518 (2020)
[33] Z-Z Zou, X-T Yu, Y-X Gong and Z-C Zhang, *Phys. Lett. A* **381**(**2**), 76 (2017)
[34] S Shuai, N Chen and B Yan, *Appl. Sci.* **10**(**16**), 5500 (2020)
[35] Y Nie, Y Li, X Wang and M Sang, *Quantum Inf. Process.* **12**(**5**), 1851 (2013)
[36] X-J Yi and J-M Wang, *Int. J. Theor. Phys.* **50**(**8**), 2520 (2011)
[37] C-P Yang, Q-P Su, Y Z and F Nori, *Phys. Rev. A* **101**(**3**), 032329 (2020)
[38] P Contreras-Tejada, C Palazuelos and J I De Vicente, *Phys. Rev. Lett.* **122**(**12**), 120503 (2019)
[39] S Bäuml, S Das, X Wang and M M Wilde, *Resource theory of entanglement for bipartite quantum channels*, arXiv:1907.04181 (2019)
[40] T Theurer, N Killoran, D Egloff and M B Plenio, *Phys. Rev. Lett.* **119**(**23**), 230401 (2017)
[41] F Shahandeh, The resource theory of entanglement, in: *Quantum correlations* (Springer, 2019) pp. 61–109
[42] M G Majumdar, *J. Appl. Math. Phys.* **7.12**, 3116 (2019)
[43] D A Lidar, I L Chuang and K Birgitta Whaley, *Phys. Rev. Lett.* **81**(**12**), 2594 (1998)
[44] P G Kwiat, A J Berglund, J B Altepeter and A G White, *Science* **290**(**5491**), 498 (2000)
[45] D Bacon, J Kempe, D A Lidar and K Birgitta Whaley, *Phys. Rev. Lett.* **85**(**8**), 1758 (2000)
[46] D A Lidar and K Birgitta Whaley, Decoherence-free subspaces and subsystems, in: *Irreversible quantum dynamics* (Springer, 2003) pp. 83–120
[47] D Gottesman, *Stabilizer codes and quantum error correction*, arXiv:quant-ph/9705052 (1997)
[48] S Bravyi and R Raussendorf, *Phys. Rev. A* **76**(**2**), 022304 (2007)
[49] R Raussendorf and H J Briegel, *Phys. Rev. Lett.* **86**(**22**), 5188 (2001)
[50] H J Briegel and R Raussendorf, *Phys. Rev. Lett.* **86**(**5**), 910 (2001)
[51] X-N Zhu and S-M Fei, *Phys. Rev. A* **90**(**2**), 024304 (2014)
[52] Y-K Bai, M-Y Ye and Z D Wang, *Phys. Rev. A* **80**(**4**), 044301 (2009)

[53] M Koashi and A Winter, *Phys. Rev. A* **69**(**2**), 022309 (2004)
[54] Z-X Jin and S-M Fei, *Quantum Inf. Process.* **16**(**3**), 77 (2017)
[55] C Di Franco, M Paternostro and M S Kim, *Phys. Rev. A* **77**(**2**), 020303 (2008)
[56] F Fröwis and W Dür, *Phys. Rev. Lett.* **106**(**11**), 110402 (2011)
[57] M Christandl, N Datta, A Ekert and A J Landahl, *Phys. Rev. Lett.* **92**(**18**), 187902 (2004)
[58] M Christandl, N Datta, T C Dorlas, A Ekert, A Kay and A J Landahl, *Phys. Rev. A* **71**(**3**), 032312 (2005)
[59] S Zippilli, J Li and D Vitali, *Phys. Rev. A* **92**(**3**), 032319 (2015)
[60] A G Fowler, A M Stephens and P Groszkowski, *Phys. Rev. A* **80**(**5**), 052312 (2009)
[61] D S Wang, A G Fowler and L C L Hollenberg, *Phys. Rev. A* **83**(**2**), 020302 (2011)
[62] H Bombín and M A Martin-Delgado, *J. Phys. A* **42**(**9**), 095302 (2009)
[63] H Bombin, *New J. Phys.* **13**(**4**), 043005 (2011)
[64] E Dennis, A Kitaev, A Landahl and J Preskill, *J. Math. Phys.* **43**(**9**), 4452 (2002)
[65] M Mhalla and S Perdrix, *Graph states, pivot minor and universality of (x, z)-measurements*, arXiv:1202.6551 (2012)
[66] R Beals, S Brierley, O Gray, A W Harrow, S Kutin, N Linden, D Shepherd and M Stather, *Proc. R. Soc. A: Math. Phys. Eng. Sci.* **469**(**2153**), 20120686 (2013)
[67] D Bruß and Norbert Lütkenhaus, *Appl. Algebra Eng. Commun. Comput.* **10**(**4–5**), 383 (2000)
[68] P Komar, E M Kessler, M Bishof, L Jiang, A S Sørensen, J Ye and M D Lukin, *Nature Phys.* **10**(**8**), 582 (2014)
[69] Z Eldredge, M Foss-Feig, J A Gross, S L Rolston and A V Gorshkov, *Phys. Rev. A* **97**(**4**), 042337 (2018)
[70] T J Proctor, P A Knott and J A Dunningham, *Networked quantum sensing,* arXiv:1702.04271 (2017)
[71] W Ge, K Jacobs, Z Eldredge, A V Gorshkov and M Foss-Feig, *Phys. Rev. Lett.* **121**(**4**), 043604 (2018)
[72] V V Kuzmin, D V Vasilyev, N Sangouard, W Dür and C A Muschik, *Npj Quantum Inf.* **5**(**1**), 1 (2019)
[73] X-W Zha, H-Y Song, J-X Qi, D Wang and Q Lan, *A genuine maximally seven-qubit entangled state*, arXiv:1110.5011 (2011)
[74] I D K Brown, S Stepney, A Sudbery and S L Braunstein, *J. Phys. A* **38**(**5**), 1119 (2005)
[75] A Borras, A R Plastino, J Batle, C Zander, M Casas and A Plastino, *J. Phys. A* **40**(**44**), 13407 (2007)